Diffusion, uptake and release of hydrogen in p-type gallium nitride: theory and experiment

S. M. Myers, A. F. Wright, G. A. Petersen, W. R. Wampler, C. H. Seager, M. H. Crawford, and J. Han

Sandia National Laboratories, Albuquerque, New Mexico 87185-1056

ABSTRACT

The diffusion, uptake, and release of H in p-type GaN are modeled employing state energies from density-function theory and compared with measurements of deuterium uptake and release using nuclear-reaction analysis. Good semiquantitative agreement is found when account is taken of a surface permeation barrier.

DISCLAIMER

in electronic image products. Images are

I. INTRODUCTION

Hydrogen is incorporated into GaN during growth by metal-organic chemical vapor deposition (MOCVD) and subsequent device processing. (See, *e.g.*, Ref. 1 and citations therein.) In the case of p-type material, the result is often a nearly complete passivation of the acceptors after growth. Reactivation is accomplished by thermal release of the H at elevated temperatures,[2-4] by minority-carrier injection at lower temperatures causing the H to transfer to a metastable, non-passivating state,[5,6] or by electron irradiation.[7,8] Thermal release is impeded by the stability of the passivated state, and this can cause retention of the H to temperatures where degradation of the semiconductor may occur. On the positive side, controlled localized repassivation of dopants may ultimately prove useful in the fabrication of devices, and repassivated has been demonstrated for p-type material through plasma and gas-phase charging.[9,10] It is therefore of technological as well as scientific interest to develop a predictive understanding of the transport, uptake, and release. Theoretical studies of H in the metastable zincblende[11,12] and equilibrium wurtzite[12] forms of GaN have indicated that the dominant charge state is H^+ or H^- depending upon the position of the Fermi level, with H^0 always being less stable. Activation energies for diffusion have also been predicted,[11,12] and while the results are not in full agreement, H^+ and H^0 are consistently found to be much more mobile than H^-. Limited experimental information on thermal release has been provided by studies concerned with thermal activation of dopants in MOCVD material, but these investigations have not included a detailed mechanistic examination of the underlying H behavior.

We are pursuing a predictive mechanistic understanding of H behavior in wurtzite GaN at temperatures sufficiently elevated for local equilibrium among H states. The initial objective is not precise modeling of experimental results through extensive parameter fitting. Rather, we seek to determine the extent to which current theoretical ideas about H in this semiconductor can account for available experimental information. To this end, theoretically predicted or independently measured parameter values are used in idealized diffusion-reaction equations to model the properties of the system, and consistency with experiment is then evaluated at a

semiquantitative level; altogether, only two adjustments are made in theoretically predicted parameters to produce agreement. A previous paper described our investigation of thermodynamic equilibrium.[10] There, state energies obtained from density-functional theory were used in thermodynamic equations to predict individual state occupancies and the combined solid solubility of the H, and the results were compared with solubilities measured by us in p- and n-type material in equilibrium with deuterium (D) gas. Good agreement was obtained by reducing the solution-state energies by 0.22 eV from *ab-initio* theoretical values.

In the present article, we describe the extension of the above theoretical modeling to include diffusion, uptake from the gas phase, and thermal release. Then, experimental results for uptake and release are reported for Mg-doped, p-type GaN films grown epitaxially on sapphire by MOCVD, and comparison is made with the theory. Semiquantitative agreement is obtained when account is taken of a strong surface-barrier effect. Preliminary findings from this work were presented elsewhere.[13]

II. THEORY

As discussed in detail elsewhere,[10] we take account of six energy minima of H within the wurtzite GaN lattice that are predicted by density-functional theory: H^+ at a N-antibonding (AB) site oriented transverse to the c-axis, H^+ at a c-axis bond-center (BC) site, H^- at an interstitial position in the open c-axis channel, H^0 in the c-axis channel, interstitial H_2, and H in a bound neutral complex with a substitutional acceptor or donor on the Ga sublattice. The theoretically obtained formation or binding energies of these states are reproduced in Table I for convenience; also included are the predicted H vibration frequencies, which are used to calculate vibrational contributions to the H chemical potential, and the diffusion activation energies for the mobile species. The total diffusion flux of H in this system is given by

$$\Phi_{dif} = -D_H^0 \frac{\partial}{\partial x}\left[H^0\right] - D_H^+ \frac{\partial}{\partial x}\left[H^+\right] - D_H^- \frac{\partial}{\partial x}\left[H^-\right] - \left(D_H^+\left[H^+\right] - D_H^-\left[H^-\right]\right)\left(\frac{1}{kT}\right)\frac{\partial}{\partial x}(E_F - E_V) \quad (1)$$

where the brackets denote atomic densities, the quantities D_H are diffusion coefficients, E_F the Fermi energy, and E_V is the energy of the valence-band edge. The final term on the right describes electric-field-driven migration resulting from spatial variation of the Fermi level. At temperatures sufficiently elevated for diffusion through the thickness of the GaN film, which is the condition of interest here, near-equilibrium is believed to exist locally between the populations of the six H states. Assuming such equilibrium, the energies and vibrational frequencies in Table I can be used in thermodynamic equations to express the concentration of each H species as a function of total H concentration [H] and Fermi energy as detailed previously.[10] The specification of the problem is then completed by three additional steps: first, the electron and hole concentrations are expressed as functions of $(E_F - E_V)$ using standard formulae and band densities of states obtained from density-functional theory; second, charge neutrality is imposed at all depths, neglecting any space charge associated with gradients in $(E_F - E_V)$; and, finally, surface boundary conditions are applied as discussed below. The solution is obtained by numerical methods discussed in the Appendix.

In Section III we will argue that experimental results indicate the presence of a surface permeation barrier characterized by second-order release kinetics. The influence of this barrier is modeled through a boundary condition on Eq. (1). In the absence of detailed knowledge of the reaction path between interstitial H in the GaN lattice and external H_2 gas, we provisionally apply a simple physical model that has been used successfully for metals; in particular, there is assumed to be rapid equilibration between interstitial solution and atomic chemisorption on the surface, and the rate-determining step is then taken to be recombinative desorption for release and dissociative adsorption for uptake from H_2 gas, both with an appreciable activation barrier. We further assume only one type of surface site, random occupation of the surface sites with no clustering, and one path for the reversible reaction $H_{sur} + H_{sur} \leftrightarrow H_2(gas)$ where H_{sur} denotes the adsorbed H atom. The net atomic flux of H through the surface into the semiconductor is then given by

$$\Phi_{sur} = -\Phi^0_{des}(\theta_{sur})^2 \exp\left(-\frac{\Delta E_{des}}{kT}\right) + \Phi^0_{ads} P^*_{gas}(1-\theta_{sur})^2 \exp\left(-\frac{\Delta E_{ads}}{kT}\right). \quad (2)$$

with

$$\frac{\theta_{sur}}{1-\theta_{sur}} = \frac{\left[H^0\right]_{x\to 0}}{[N]} \exp\left(\frac{\Delta E_{sur}}{kT}\right). \quad (3)$$

where θ_{sur} is the fractional occupancy of surface sites, ΔE_{des} is the activation energy for recombinative desorption, P^*_{gas} is the fugacity (equal to pressure at low pressures) of the gas, ΔE_{ads} is the activation energy for dissociative adsorption, Φ^0_{des} and Φ^0_{ads} are constants, $\left[H^0\right]_{x\to 0}$ is the atomic density of neutral H in interstitial solution in the vicinity of the surface, [N] is the atomic density of N in GaN, and ΔE_{sur} is the change in the nonconfigurational part of the Gibbs free energy when one H atom is transferred from neutral interstitial solution to the surface. In Eq. (2), the first term on the right describes release from solution, while the following term gives the rate of uptake from H_2 gas. As noted above, interstitial H in GaN is theoretically predicted to exist in six states, and at the elevated temperatures of interest the populations of these states are expected to remain in mutual equilibrium. Hence, Eq. (3) could be formulated in terms of any of these concentrations. We use H^0 as a matter of convenience because of its electrical neutrality and relatively small concentration, thereby avoiding a Fermi-level dependence and the nonlinearities associated with saturation. In the case of the boundary at the interface with the substrate, we assume $\Phi_{sur} = 0$.

The parameters in Eqs. (2) and (3) are constrained by the requirement that, when Φ_{sur} =0, the resulting relation between $\left[H^0\right]_{x\to 0}$ and P^*_{gas} must conform to the equilibrium solubility. If the solubility is independently known, then specifying the parameters for release determines those for uptake, and vice versa. In a previous paper, we reported that the solubility of the neutral species is given approximately by[10]

$$\left[H^0\right]^{sol} = \left(6.6\times 10^{19}\,\text{atoms/cm}^3\right)\left(\frac{P^*}{1\,\text{bar}}\right)^{1/2} \exp\left(-\frac{2.48\text{eV}}{kT}\right) \quad (4)$$

for the protium isotope based on a combination of theoretical and experimental information. The result for deuterium is essentially the same, with an activation energy of 2.50 eV and a prefactor of 6.2×10^{19} atoms/cm^3.

The above theoretical formalism is used in Section III to model our experimental results on thermal release and uptake from the gas phase. In these calculations, the theoretical numbers in Table I are employed without fitting to treat diffusion and the relative occupancies of the H solution states, making use of the aforementioned equilibrium relations between the state concentrations. The model calculation is carried out for the deuterium isotope (D), which was utilized in most of our experiments, and consequently the tabulated H frequencies are divided by $\sqrt{2}$. In the absence of theoretical or experimental information on the diffusion prefactors, a representative interstitial-diffusion value of 10^{-3} cm^2/s is used. The ionization level of the Mg acceptor is taken to be 0.16 eV above the valence-band edge on the basis of published experimental results. (See, *e.g.*, Ref. 14 and citations therein.).

The surface-barrier parameters in Eqs. (2) and (3) are evaluated largely from experimental information, including other published work as well as the results in Section III, with limited theoretical input. The method of evaluation will now be outlined with reference to the energy diagram in Fig. 1. The prefactor Φ^0_{des} is estimated by taking the product of the areal density of surface sites and a trial frequency; the former quantity is equated to the atomic density of the unreconstructed GaN (0001) surface, 1.14×10^{15} atoms/cm^3, while the latter is taken to be $\sim10^{14}$ s^{-1} in accord with measured vibration frequencies of surface H,[15] giving $\Phi^0_{des} \sim 10^{29}$ atoms/cm^2/s. The energy difference between D^0 in solution and external D_2 gas is 2.40 eV per atom based on our previous theoretical and experimental study of D solubility in GaN.[10] (This difference between zero-temperature formation energies differs slightly from the elevated-temperature activation energy in Eq. (4).) For purposes of later discussion, Fig. 1 also shows the relative formation energies of H^+ and the neutral MgH center, as derived from the theoretical information in Table I. The activation barrier for recombinative desorption E_{des} is estimated by analyzing published measurements of the release of adsorbed D in ultrahigh-

vacuum during temperature ramping.[16] With a ramp rate of 3 °C/s, the peak in the release occurred at 352°C; assuming that the release is described by the first term on the right in Eq. (2), this implies $E_{des} \approx 1.8$ eV. Still undermined is the parameter ΔE_{sur} in Eq. (3), which will be evaluated in Section III by fitting to our experimental data on thermal release. In doing this we will assume that ΔE_{sur} is to first order independent of temperature, or, equivalently, that that interstitial D^0 and surface D have similar vibrational modes. Lastly, the rate of uptake from D_2 gas will be predicted without further adjustment of parameters by imposing the equilibrium condition of Eq. (4) as discussed above.

III. EXPERIMENTS AND COMPARISON WITH THEORY

P-type GaN was grown epitaxially on sapphire by MOCVD as described elsewhere.[17] The films were 1.5-2 μm thick, and included an intermediate, undoped layer extending ~0.2-0.4 μm from the substrate interface. The p-type region was doped with Mg to a concentration of approximately 5×10^{19} atoms/cm^3 as measured by secondary-ion mass spectrometry (SIMS). After thermal release of the grown-in H, Hall-effect measurements typically showed a room-temperature hole concentration near 4×10^{17} cm^{-3}. Oxygen and C impurities were present after growth at a concentration of ~10^{17} atoms/cm^3 as measured by SIMS.

Most of the uptake and release experiments employed deuterium, which was introduced after removing the grown-in H. This initial outgassing was accomplished by annealing at 900°C for 1 hour in a quartz furnace tube that was continuously ion-pumped to a vacuum of ~10^{-7} Torr; SIMS subsequently showed a residual H concentration of ~10^{17} atoms/cm^3, or two orders of magnitude below the concentrations of D subsequently investigated. The D was introduced by heating in research-grade D_2 gas in the aforementioned furnace tube, usually at 700°C for 4 hours under a pressure of 0.88 bar; the anneal was terminated by removing the furnace from the tube in ~1 s with the gas still in place. This treatment was found to increase the resistivity of the material from 2.6 Ω-cm to 1.4×10^4 Ω-cm, indicating a nearly complete neutralization of the

Mg acceptors. Thermal release of the D was then investigated during sequences of isothermal anneals carried out at 600-800°C in an ion-pumped vacuum of $\sim 10^{-7}$ Torr.

The concentration of D in the GaN layers was determined by nuclear-reaction analysis using the ^{3}He-induced reaction D(^{3}He,p)^{4}He as detailed elsewhere.[18] The proton yield from this reaction was measured as a function of ^{3}He energy from 0.4 to 1.6 MeV, and the depth distribution of the D was then extracted by deconvolution[18] using published results for the nuclear cross section[19] and He stopping rate.[20] In the deconvolution procedure, the D concentration-versus-depth profile is represented by contiguous straight-line segments with depth intervals chosen to accommodate regions of rapid variation such as the sample surface and the base of the p-type region. The concentrations at the termini of these segments are then adjusted so as to fit the measured energy-dependent proton yield in a least-squares sense. The method is exemplified in Fig. 2, which shows the experimental data and derived concentration profile for a specimen that was charged in D_2 gas at 700°C for 5 hours under a pressure of 0.88 bar, a treatment producing nearly complete passivation of the Mg and high electrical resistivity. The step in D concentration near 1 μm corresponds to the base of the Mg-doped region.

The D concentration in the doped region of the film in Fig. 2, about 2×10^{19} atoms/cm^3, is substantially smaller than the Mg concentration of approximately 5×10^{19} atoms/cm^3, not withstanding the large reduction in electrical conductivity. As discussed in greater detail elsewhere,[10] we attribute this difference to a characteristic of MOCVD-type GaN that is also believed responsible for the rather general observation of hole concentrations smaller than predicted for the nominal doping level: a combination of some electrically inactive Mg and the presence of compensating defect-related donors. As noted in Ref. 10, the reduced saturation concentration of D and the aforementioned room-temperature hole concentration of 4×10^{17} cm^{-3} after H release can be simultaneously accounted for in the theoretical model by taking the concentration of electrically active Mg to be 2.4×10^{19} atoms/cm^3 and the

concentration of shallow donors 2×10^{19} cm^{-3}. These values will be used hereinafter in our treatment of uptake and release.

Isothermal-release data obtained by the above procedure at 700, 800, and 900°C are given by the solid circles in Fig. 3, where the retained fraction of D in the film is plotted as a function of anneal time. Also included is a datum for the release of grown-in H during a rapid thermal anneal of 7 s at 1000°C in flowing N_2 gas. This particular treatment is one used for electrical activation of device structures. The retained H fraction in this case was estimated using the infrared absorption of the Mg-H complex at 3125 cm^{-1}; the area of the absorption peak decreased by approximately 75% during the anneal, giving a retained fraction of 0.25.

The measured release rates in Fig. 3 are far smaller that expected for diffusion-limited flow to the surface and prompt release. This is illustrated in Fig. 4, where the experimental release data for 700°C are compared with the prediction of the theoretical model of Section II using the parameter values in Table I and a zero-concentration surface boundary condition; the disparity in rates is seen to be more than six orders of magnitude. We take this as one indication of a surface permeation barrier.

A second indicator of the rate-determining step is the kinetics of release, as reflected in the shape of the time dependences in Fig. 3. According to the theoretical model, the release rate is in general a complicated function of anneal time as a result of the interplay between matrix diffusion and surface recombination, the variation of Fermi level with D concentration, and nonlinearities occurring near saturation D passivation of Mg acceptors. When, however, the release is limited primarily by the surface barrier rather than diffusion, and when in addition the release has advanced to the point where [D] << [Mg], the behavior is simpler. Under these conditions [H] is essentially uniform in the material, and for a given temperature there is a nearly fixed proportionality between [H] and surface occupancy θ_{sur}. (An addition requirement for the latter property is that $\theta_{sur} << 1$, so that the numerator $1-\theta_{sur}$ in Eq. (3) is close to 1. This condition is satisfied when the principally occupied solution states, D^+ and MgD, are lower in

energy than the surface states as depicted in Fig. 1. Such is found to be the case when we evaluate ΔE_{sur}, as discussed below.) One then obtains from Eqs. (2) and (3)

$$\frac{d[D]}{dt} \propto -[D]^2 \tag{5}$$

or

$$\frac{d}{dt}\left(\frac{1}{[D]}\right) = \text{constant}. \tag{6}$$

In Fig. 5 the release data for 800°C are replotted in a format where Eq. (5) gives a straight line, and the experimental results are seen to obey this dependence at longer times. Since we are unaware of other plausible scenarios that would produce such second-order release kinetics, this result is taken as further evidence for a surface-barrier effect.

The solution of Eqs. (1)-(3) was fitted to the experimental data in Fig. 3 by adjusting a single parameter, ΔE_{sur}, with all other quantities being independently evaluated as discussed in Section II. The small difference between the model predictions for D and H was ignored in this analysis. The results are given by the solid curves in Fig. 3 and the single solid curve in Fig. 5, which are seen to provide a good semiquantitative description of the entire body of release data. The fitted value of ΔE_{sur} is – 1.57 eV, which gives the relative state energies shown in Fig. 1.

The rate of uptake from D_2 gas was also examined experimentally, but in less detail. Here we report two approximate rates: for 500°C and a D_2 pressure of 0.88 bar, $\Phi_{sur} \approx 3\times10^{11}$ atoms/cm^2/s; and, for 700°C and the lower pressure 0.013 bar, again about 3×10^{11} atoms/cm^2/s. With the parameters of the theoretical model already determined, predictions can be made for comparison with these values. The theoretical result for 500°C is 3.3×10^{10} atoms/cm^2/s, an order of magnitude smaller than observed; for 700°C at the reduced pressure, we obtain 1.6×10^{11} atoms/cm^2/s, about one-half the experimental value.

The theoretical model can be used to calculate the increase in room-temperature hole concentration as H or D is progressively removed from the p-type GaN, which is the property of

most immediate technological interest. Results are shown in Fig. 6 for the conditions of isothermal D release treated in Fig. 5. The asymptotically approached concentration is 4×10^{17} cm^{-3}, substantially less than the value of 2×10^{10} cm^{-3} for fully ionized Mg due to the appreciable ionization energy of this acceptor, 0.16 eV for $E_F = E_V$.

IV. DISCUSSION AND CONCLUSIONS

From the comparisons between experiment and theory discussed in Section III and those relating to thermodynamic equilibrium reported in Ref. 10, we conclude that that current theoretical understanding of H behavior in p-type GaN is largely compatible with experimental information when account is taken of a surface permeation barrier. Moreover, we consider the experimental evidence for the existence of the surface barrier to be strong. With regard to the detailed physical assumptions made in the theoretical model, those seeming most subject to question relate to the surface barrier. While the second-order kinetics evidenced in Fig. 5 support the identification of H-H recombination as the rate-determining step, the assumption of an unreconstructed surface with a single type of H site and the neglect of the effect of adsorbates such as O may prove to be very crude approximations. Furthermore, the influences of adsorbates and reconstruction may depend sensitively upon temperature and ambient. Additional experimentation is needed in this area, along with *ab-initio* theoretical treatments of the surface processes.

Pending systematic studies of the variability of the surface barrier, we consider some of the limited information currently available. Figure 3 includes data from both high-vacuum and N_2-ambient annealing, and while the experiments were carried out at different temperatures, the semiquantitative consistency with theory for the same parameter values suggests that the strength of the barrier effect is not dramatically affected by the flowing N_2. It should also be noted, however, that adsorbate effects in gaseous ambients may be more prevalent at temperatures less elevated than 1000°C. Comparison can also be made between the theoretical model and published experimental results on the electrical activation of p-type material where the heat

treatment was carried out in flowing N_2 gas.[4] That study employed Mg-doped GaN grown by MOCVD as in the present study, and from detailed Hall-effect measurements the investigators deduced a maximum concentration of electrically active Mg and a concentration of compensating donors insignificantly different from those used by us; they obtained 2.3×10^{19} atoms/cm^3 and 0.39×10^{19} cm^{-3}, respectively, whereas our corresponding values are 2.4×10^{19} and 0.4×10^{19}. The activation anneals in that study were performed at 600, 700, or 775°C with a duration of 5 minutes. Figure 7 shows the resulting room-temperature hole concentrations as extracted experimentally and as predicted by the model. There is seen to be good semiquantitative agreement for 700 and 775°C, whereas the anneal at 600°C produced substantially less activation than predicted. We similarly modeled the isochronal series of activation anneals reported in Ref. 2, and again found good agreement with the observed electrical properties at 700°C and above, while at 600°C and below the observed activation rate is smaller than predicted. These greater disparities at the lower temperature may reflect changes in the surface barrier, possibly due to adsorbates.

The model calculations in Figs. 3 and 6 shed light on a widely noted characteristic of the thermal activation of p-type GaN, namely, that while increases in conductivity appear after heating at temperatures as low as 500°C, a large fraction of the grown-in H can remain to 900°C or even higher. A key insight from our calculations is that, when the Mg is almost fully passivated at zero time, the rate of H release decreases extremely rapidly as the H concentration goes down. This effect arises largely from the rapid variation of H chemical potential as the passivation of Mg centers approaches completion, and is amplified by the second-order kinetics of the surface release. Consequently, for example, during an isochronal series of anneals, the first increment of H emerges at an early stage with an accompanying increase in hole concentration, while remnants of the H remain to a much higher temperature.

In our view, the mechanism-based modeling described here and in Ref. 10 has the potential ultimately for quantitative prediction of H behavior at the elevated temperatures where local equilibrium among states is expected. If achieved, this would have benefits for device

processing. At lower temperatures where the activated transitions between H states are not rapid, making inappropriate the assumption of local equilibration, substantially more theoretical work and experimental verification remains to be done.

ACKNOWLEDGEMENTS

The SIMS measurements of this study were carried out by Charles Evans & Associates, Redwood City, California. This work was supported by the U. S. Department of Energy under Contract DE-AC04-94AL85000, under the auspices of the Office of Basic Energy Sciences. Sandia National Laboratories is a multiprogram laboratory operated by Sandia Corporation, a Lockheed Martin Company, for the United States Department of Energy.

APPENDIX: NUMERICAL SOLUTION OF THE DIFFUSION EQUATION

Substituting Eq. (1) into the continuity relation

$$\frac{\partial[H]}{\partial t} = -\frac{\partial}{\partial x}\Phi_{dif} \tag{A1}$$

gives the diffusion equation

$$\begin{aligned}\frac{\partial[H]}{\partial t} = {} & D_H^0 \frac{\partial^2}{\partial x^2}\left[H^0\right] \\ & + D_H^+ \frac{\partial}{\partial x}\left(\frac{\partial}{\partial x}\left[H^+\right] + \left[H^+\right]\left(\frac{1}{kT}\right)\frac{\partial E_F}{\partial x}\right) \\ & + D_H^- \frac{\partial}{\partial x}\left(\frac{\partial}{\partial x}\left[H^-\right] - \left[H^-\right]\left(\frac{1}{kT}\right)\frac{\partial E_F}{\partial x}\right)\end{aligned} \tag{A2}$$

where $[H^0]$, $[H^+]$, and $[H^-]$ are function of [H] as given by equilibrium relations discussed elsewhere,[10] and $(E_F - E_V)$ has been replaced by E_F for compactness. In order to solve Eq. (A2) numerically, x is discretized with interval Δx to obtain values x_i with i = 1 to N and $x_1 = 0$, and

the derivatives with respect to x are then evaluated using a finite-element approximation. For i = 2 to N–1,

$$\left.\frac{\partial^2}{\partial x^2}\left[H^0\right]\right|_{x=x_i} \approx \frac{1}{(\Delta x)^2}\left(\left[H^0\right]_{i-1} + \left[H^0\right]_{i+1} - 2\left[H^0\right]_i\right) \tag{A3}$$

and

$$\left.\frac{\partial}{\partial x}\left(\frac{\partial}{\partial x}\left[H^+\right] + \left[H^+\right]\left(\frac{1}{kT}\right)\frac{\partial E_F}{\partial x}\right)\right|_{x=x_i} \approx \frac{1}{(\Delta x)^2}\left(\left[H^+\right]_{i-1} + \left[H^+\right]_{i+1} - 2\left[H^+\right]_i\right)$$
$$+\frac{1}{(\Delta x)^2}\left(\left(\frac{\left[H^+\right]_i + \left[H^+\right]_{i+1}}{2}\right)\left(\frac{E_{F,i+1} - E_{F,i}}{kT}\right) - \left(\frac{\left[H^+\right]_{i-1} + \left[H^+\right]_i}{2}\right)\left(\frac{E_{F,i} - E_{F,i-1}}{kT}\right)\right) \tag{A4}$$

with a similar relation for $[H^-]$. The surface boundary condition corresponding to Eq. (2) is implemented in two steps. First, zero diffusive flow is imposed at the surface by using a reflecting boundary; this is done by applying Eqs. (A3), (A4), and the H^- analog of Eq. (A4) to the case i=1 with the substitutions $[H^0]_{i-1} = [H^0]_{i+1}$, $[H^+]_{i-1} = [H^+]_{i+1}$, and $[H^-]_{i-1} = [H^-]_{i+1}$. Then, H is introduced at flux Φ_{sur} by adding to the time derivative of $[H]_1$ the term $2\Phi_{sur}/\Delta x$; the factor of 2 in this term can be regarded as compensating for one-half of the injected H going into the mirror-image profile. In the case of the boundary at the substrate interface, the same procedure is applied with $\Phi_{sur} = 0$.

In practice, we find it useful to replace Eq. (A4) and its H^- analog with equations that reduce to the same form in the limit $\Delta x \to 0$, but which also provide an exact description of equilibrium between depths x_i and x_{i+1} regardless of whether the increment in E_F is infinitesimal. This makes the solution more accurate for a given value of Δx and allows a seamless treatment of steps in dopant concentration. The equation used in place of Eq. (A4) is

$$\frac{\partial}{\partial x}\left(\frac{\partial}{\partial x}\left[H^+\right]+\left[H^+\right]\left(\frac{1}{kT}\right)\frac{\partial E_F}{\partial x}\right)\Bigg|_{x=x_i} \approx \frac{1}{(\Delta x)^2}\left(\left[H^+\right]_{i-1}\exp\left(\frac{-E_{F,i}+E_{F,i-1}}{2kT}\right)\right)$$
$$+\frac{1}{(\Delta x)^2}\left[H^+\right]_{i+1}\exp\left(\frac{E_{F,i+1}-E_{F,i}}{2kT}\right) \qquad \text{(A5)}$$
$$-\frac{1}{(\Delta x)^2}\left[H^+\right]_i\left(\exp\left(\frac{E_{F,i}-E_{F,i-1}}{2kT}\right)+\exp\left(\frac{-E_{F,i+1}+E_{F,i}}{2kT}\right)\right)$$

The result of the above manipulations is a system of coupled ordinary differential equations of the generic form

$$\frac{\partial[H]_i}{\partial t} = f\left([H]_{i-1},[H]_i,[H]_{i+1}\right). \qquad \text{(A6)}$$

The solution is obtained using a stiff integrator with banded Jacobian.[21]

REFERENCES

1. S. J. Pearton, J. C. Zolper, R. J. Shul, and F. Ren, J. Appl. Phys. **86**, 1 (1999).
2. S. Nakamura, T. Mukai, M. Senow, and N. Iwasa, Jpn. J. Appl. Phys. **31**, L139 (1992).
3. C. Yuan, T. Salagaj, A. Gurary, P. Zawadzki, C. S. Chern, W. Kroll, R. A. Stall, Y. Li, M. Schurman, C.-Y. Hwang, W. E. Mayo, Y. Lu, S. J. Pearton, S. Krishnankutty, and R. M. Kolbas, J. Electrochem. Soc., **142**, L163 (1995).
4. W. Götz, N. M. Johnson, J. Walker, D. P. Bour, and R. A. Street, Appl. Phys. Lett. **68**, 667 (1996).
5. S. J. Pearton, J. W. Lee, and C. Yuan, Appl. Phys. Lett. **68**, 2690 (1996).
6. M. Miyachi, T. Tanaka, Y. Kimura, and H. Ota, Appl. Phys. Lett. **72**, 1101 (1998).
7. M. Inamori, H. Sakai, T. Tanaka, H. Amano, and I. Akasaki, Jpn. J. Appl. Phys. **34**, 1190 (1995).
8. X. Li and J. J. Coleman, Appl. Phys. Lett. **69**, 1605 (1996).
9. M. S. Brandt, N. M. Johnson, R. J. Molnar, R. Singh, and T. D. Moustakas, Appl. Phys. Lett. **64**, 2264 (1994).
10. S. M. Myers, A. F. Wright, G. A. Petersen, C. H. Seager, W. R. Wampler, M. H Crawford, and J. Han, submitted to J. Appl. Phys.
11. J. Neugebauer and C. G. Van de Walle, Phys. Rev. Lett. **75**, 4452 (1995).
12. A. F. Wright, Phys. Rev. B **60**, R5101 (1999).
13. S. M. Myers, A. F. Wright, G. A. Petersen, C. H. Seager, M. H. Crawford, W. R. Wampler, and J. Han, MRS Internet J. Nitride Semicond. Res. 5S1, W9.4 (2000).
14. P. Kozodoy, H. Xing, S. P. DenBaars, U. K. Mishra, A. Saxler, R. Perrin, S. Elhamri, and W. C. Mitchel, J. Appl. Phys. **87**, 1832 (2000).
15. V. J. Bellitto, Y. Yang, B. D. Thoms, D. D. Koleske, A. E. Wickenden, and R. L. Henry, Surf. Sci. **442**, L1019 (1999).
16. R. Shekhar and K. F. Jensen, Surf. Sci. **381**, L581 (1997).

17. J. Han, T.-B. Ng, R. M. Biefield, M. H. Crawford, and D. M. Follstaedt, App. Phys. Lett. **71**, 3114 (1997).

18. S. M. Myers, G. R. Caskey, Jr., D. E. Rawl, Jr., and R. D. Sisson, Jr., Metall. Trans. A **14**, 2261 (1983).

19. W. Möller and F. Besenbacher, Nucl. Instrum. Meth. **168**, 111 (1980).

20. J. F. Ziegler, Helium Stopping Powers and Ranges in All Elemental Matter (Pergamon, New York, 1977).

21. A. C. Hindmarsh, in Scientific Computing (IMACS/North Holland, 1983), pp. 55-64. The particular code used is DDEBDF, which has been documented by L. F. Shampine and H. A. Watts, "Design of a User Oriented Package of ODE Solvers" (Sandia National Laboratories, Internal report SAND79-2374, 1980).

TABLE I. Properties of H in GaN at zero temperature from density-functional theory.[10] The formation-energy reference state comprises the neutral H atom in vacuum and GaN with electronic dopants neutral. Vibrational frequencies are divided by the speed of light, c.

Species	Formation energy at $E_F=E_V$ (eV / H atom)	*Diffusion activation energy (eV)	Vibration frequency / c (cm^{-1})
H^0	+0.34	0.6	692 (c-axis)
			816 (⊥ c-axis, 2 modes)
H^+(AB)†	–2.67	0.7	2970 (stretch)
			847 (bend, 2 modes)
H^+(BC)‡	–2.67	0.7	3420 (stretch)
			502 (bend, 2 modes)
H^-	+1.52	1.6	1216 (c-axis)
			1406 (⊥ c-axis, 2 modes)
H_2	–1.40		4235 (mol. stretch)
			1091 (displ. c-axis)
			1384 (displ. ⊥ c-axis, 2 modes)
			1012 (shear ⊥ c-axis, 2 modes)
	Binding energy # (eV)		
MgH	–0.7		3284 (stretch)
			937 (bend, 2 modes)
SiH	–0.3		1739 (stretch)
			1302, 1427 (bend)

* For diffusion along the c-axis

† Nitrogen antibonding site

‡ Bond-center site

Relative to ionized dopant and oppositely charged H

FIGURE CAPTIONS

1. Diagram of surface-related H energies. Relative energies are shown to scale.
2. Depth profile of D as obtained from nuclear-reaction analysis.
3. Measured release of gas-charged D or grown in ^{1}H during isothermal annealing and predictions of the fitted theoretical model. The p-doped region extends from the surface to a depth of about 1.1 μm in the 1.6-μm GaN film as shown by SIMS.
4. Measured D release at 700°C compared with theoretical predictions assuming no surface permeation barrier.
5. Deuterium release at 800°C plotted in a format to exhibit second-order release kinetics.
6. Theoretically predicted increase in room-temperature hole concentration resulting from isothermal release of D.
7. Thermal activation of p-type GaN reported in Ref. 4 compared with model predictions.

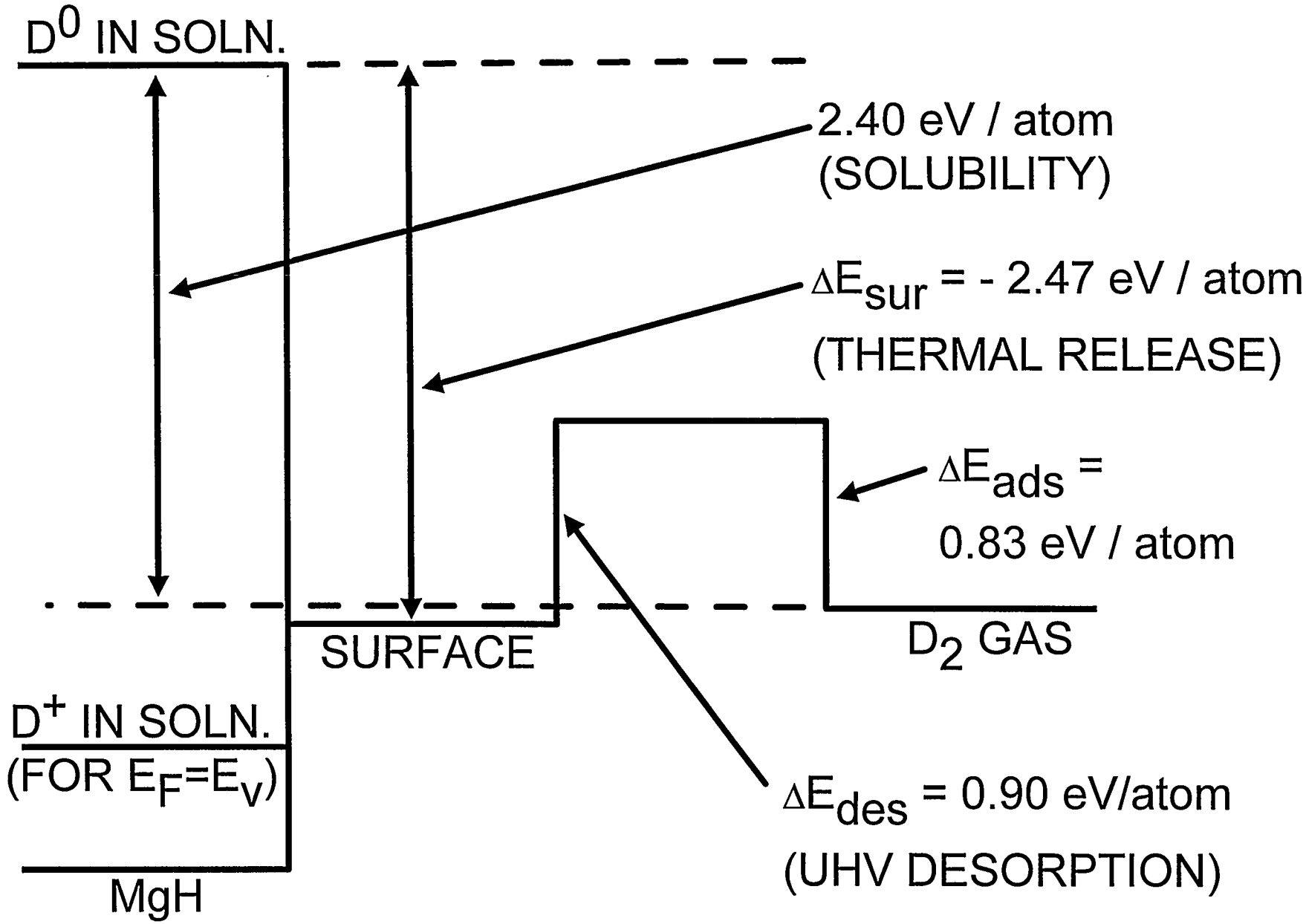
D0 IN SOLN.
2.40 eV / atom
(SOLUBILITY)
ΔEsur = - 2.47 eV / atom
(THERMAL RELEASE)
ΔEads =
0.83 eV / atom
SURFACE
D2 GAS
D+ IN SOLN.
(FOR EF=EV)
ΔEdes = 0.90 eV/atom
(UHV DESORPTION)
MgH

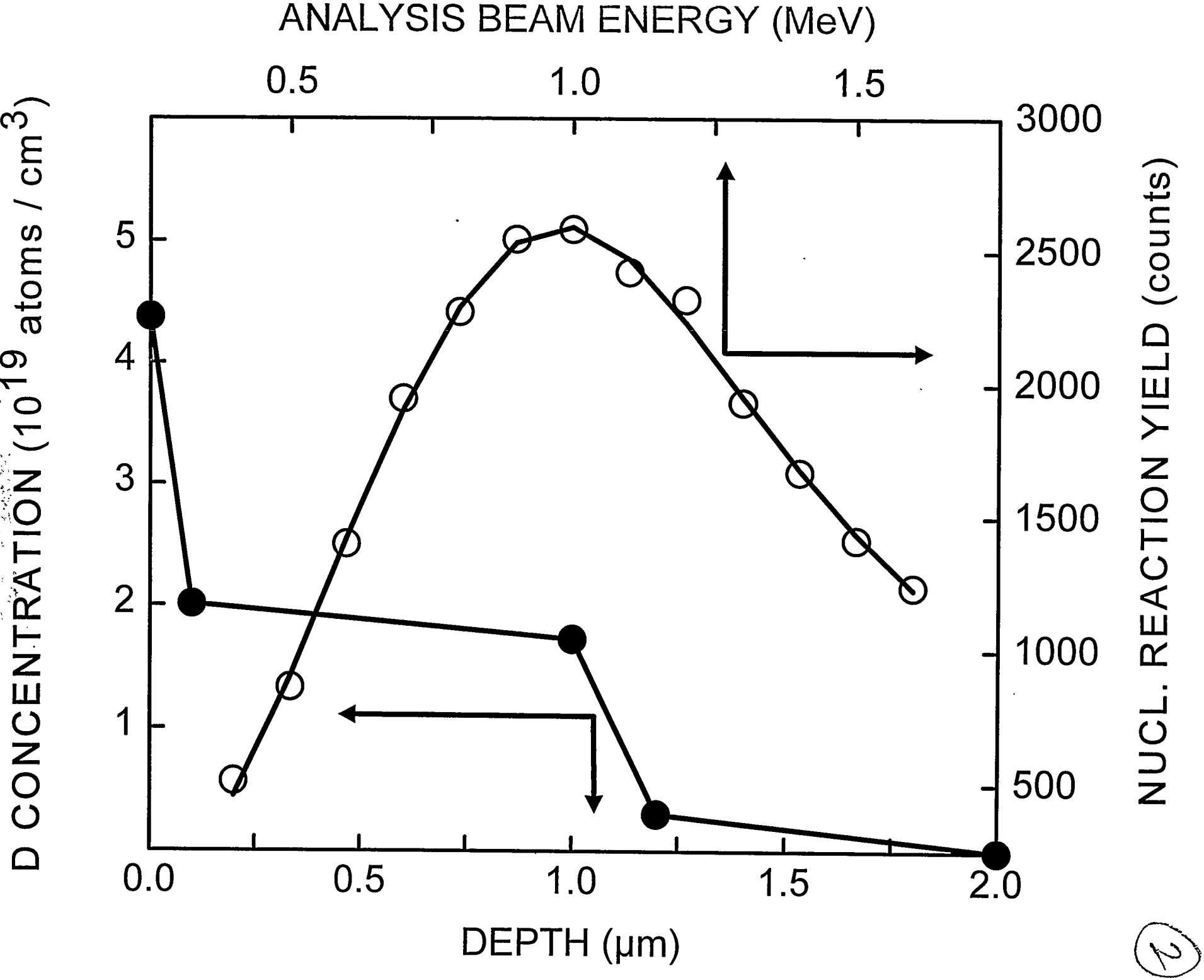
ANALYSIS BEAM ENERGY (MeV)
0.5
1.0
1.5
D CONCENTRATION (10^{19} atoms / cm^3)
NUCL. REACTION YIELD (counts)
3000
2500
2000
1500
1000
500
5
4
3
2
1
0.0
0.5
1.0
1.5
2.0
DEPTH (μm)

(1)

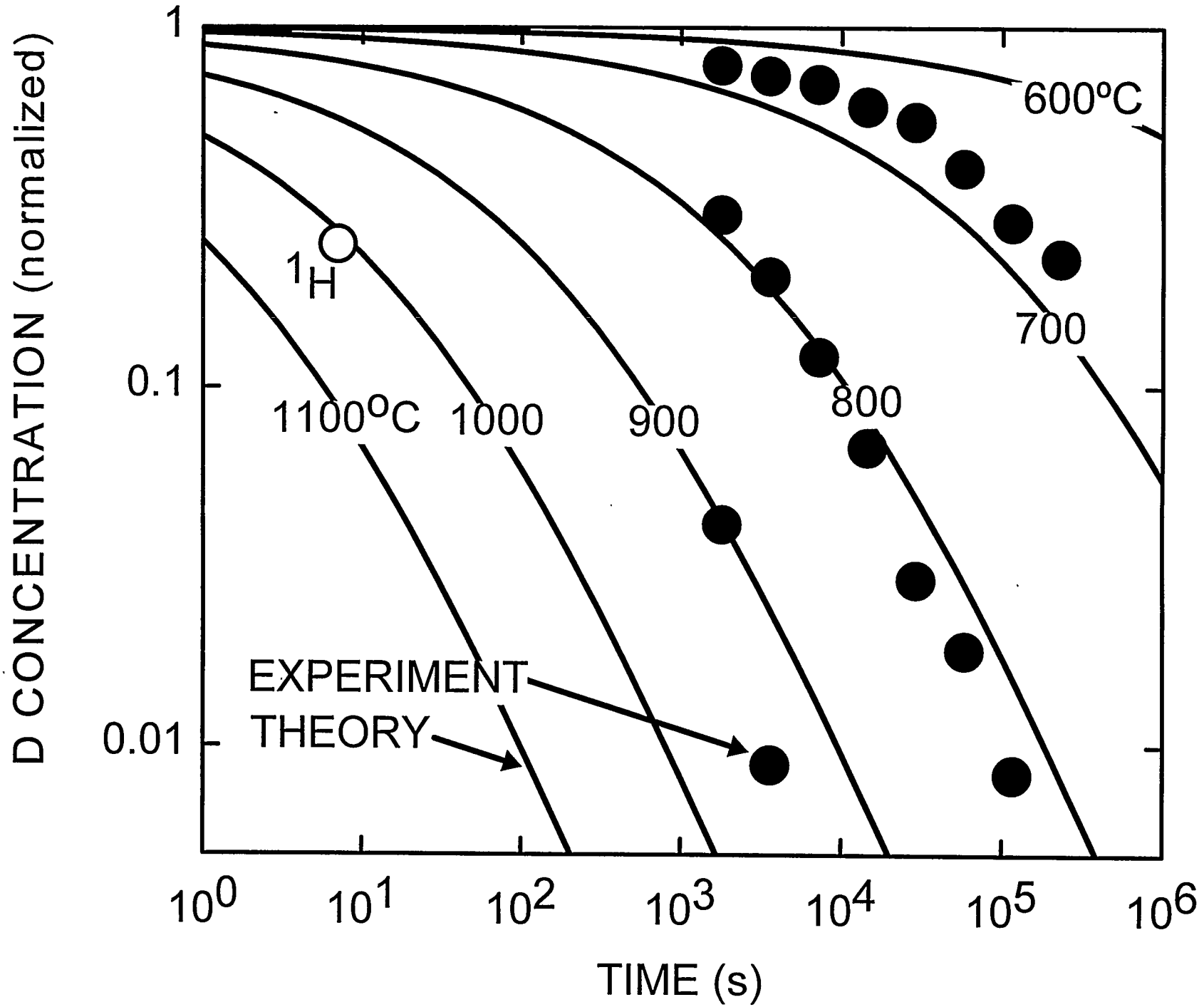
D CONCENTRATION (normalized)
1
0.1
0.01
10^0
10^1
10^2
10^3
10^4
10^5
10^6
TIME (s)
600°C
700
800
900
1000
1100°C
^1H
EXPERIMENT
THEORY

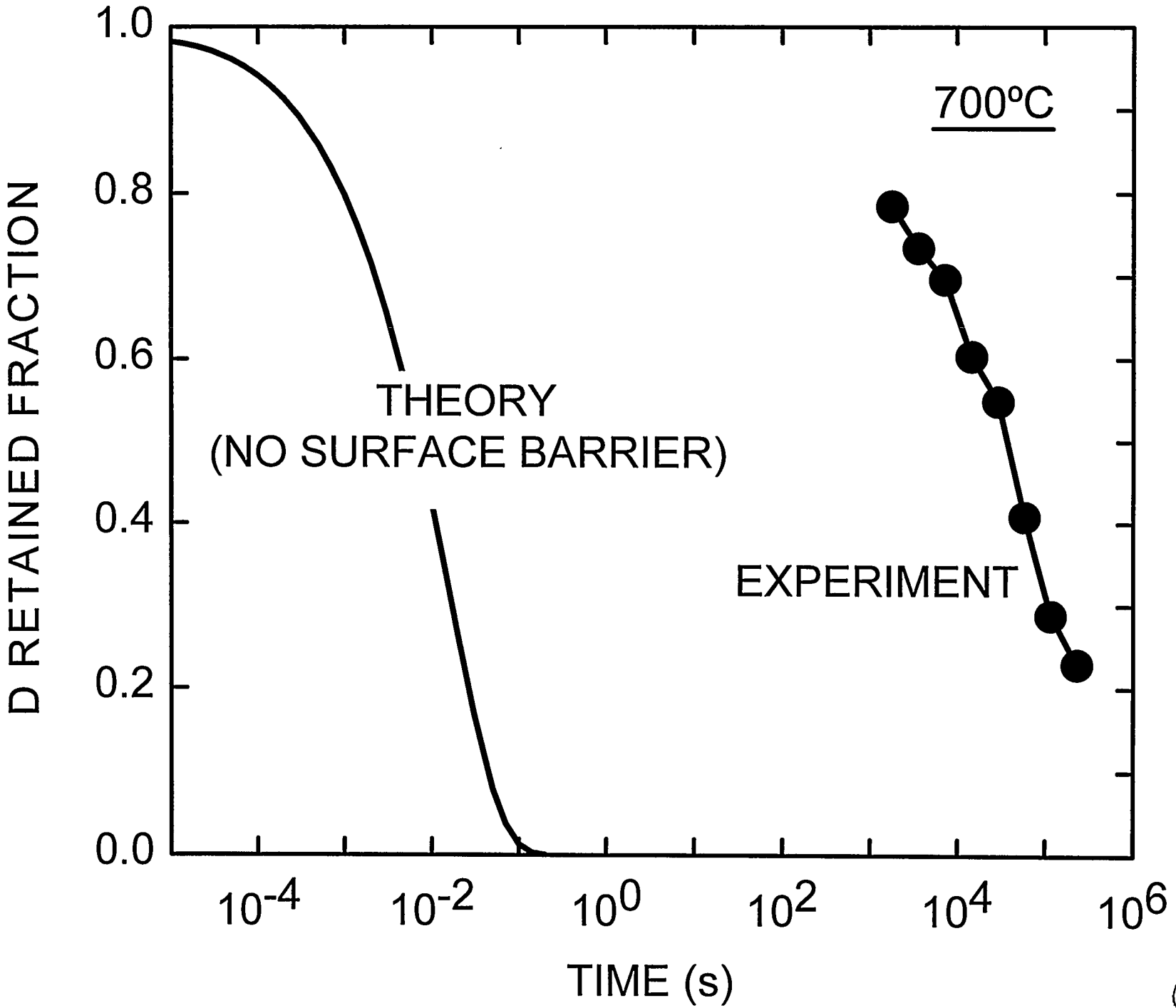
1.0
0.8
0.6
0.4
0.2
0.0
D RETAINED FRACTION
700°C
THEORY
(NO SURFACE BARRIER)
EXPERIMENT
10^{-4}
10^{-2}
10^{0}
10^{2}
10^{4}
10^{6}
TIME (s)

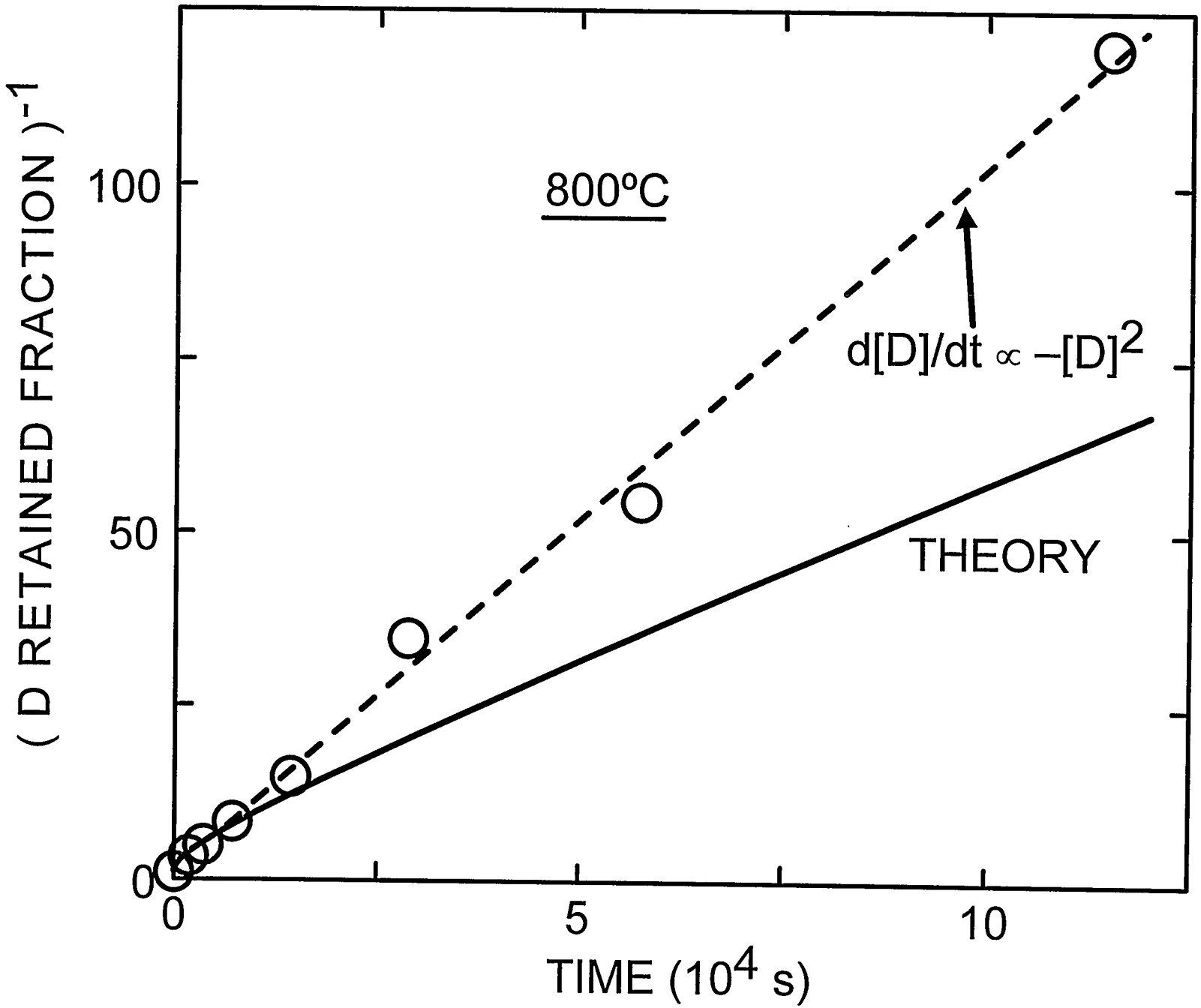
(D RETAINED FRACTION)$^{-1}$
100
50
0
0
5
10
TIME (10^4 s)
800ºC
d[D]/dt ∝ –[D]^2
THEORY

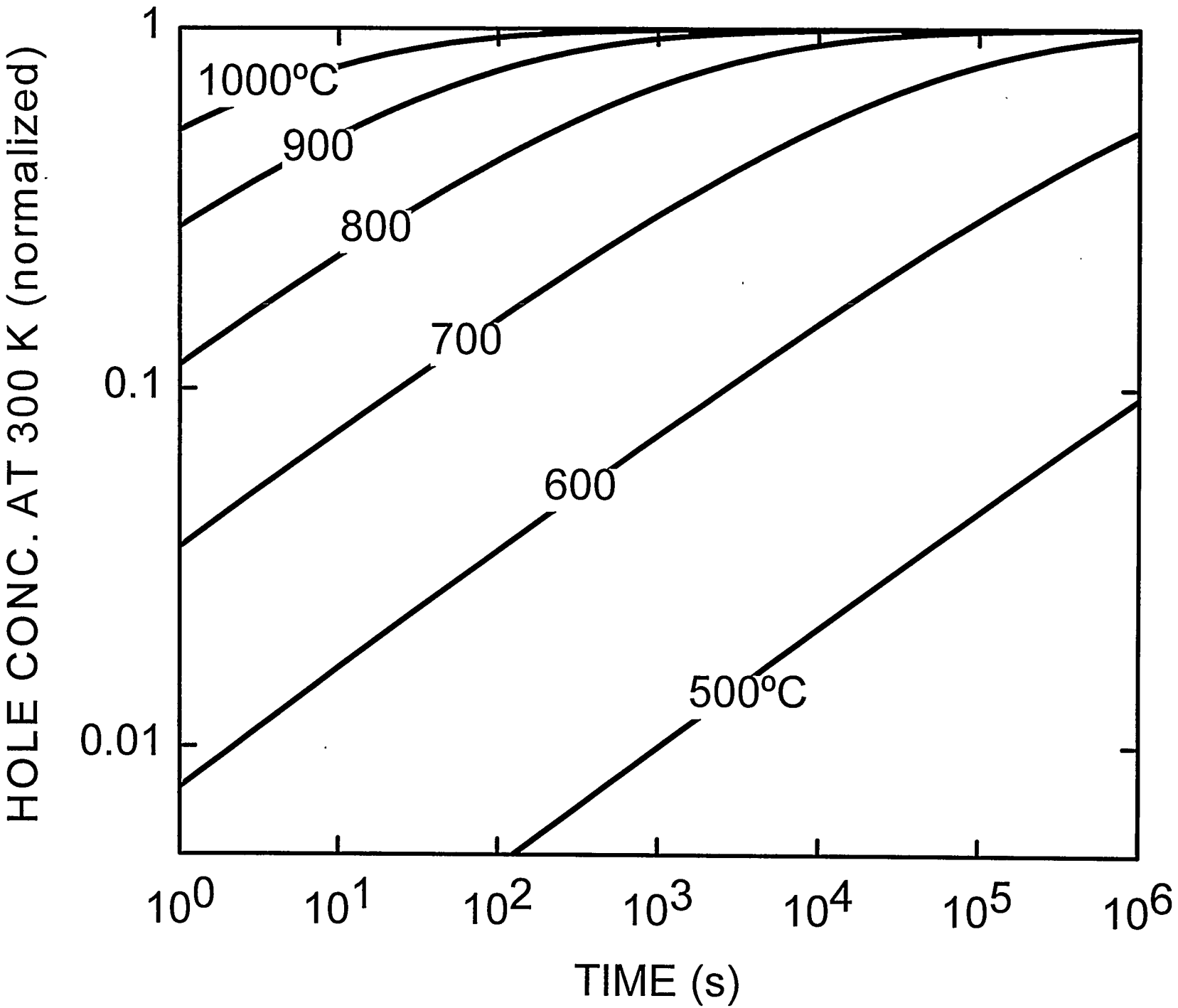
HOLE CONC. AT 300 K (normalized)
1
0.1
0.01
1000°C
900
800
700
600
500°C
10^0
10^1
10^2
10^3
10^4
10^5
10^6
TIME (s)

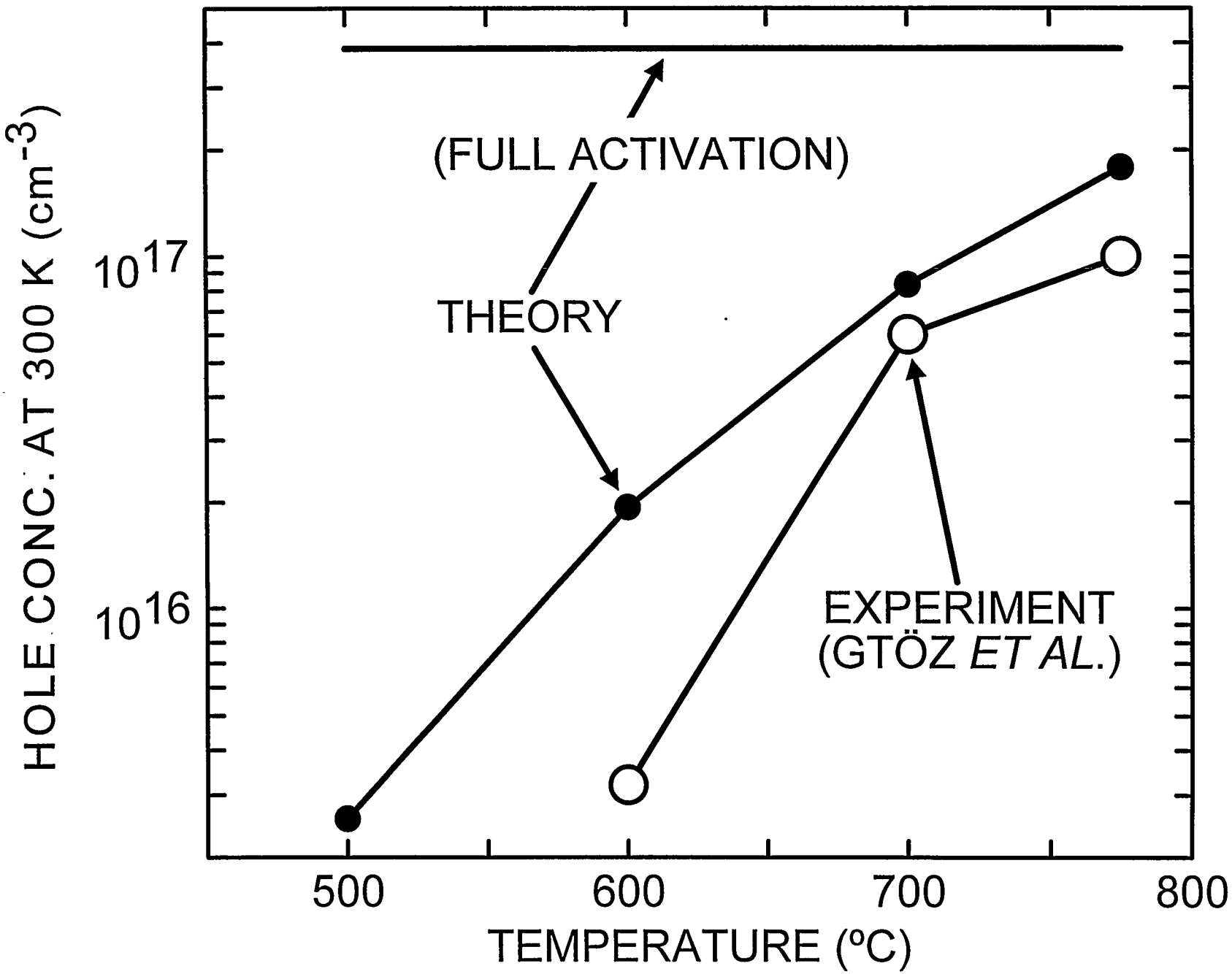
HOLE CONC. AT 300 K (cm^{-3})
10^{17}
10^{16}
(FULL ACTIVATION)
THEORY
EXPERIMENT
(GTÖZ *ET AL.*)
500
600
700
800
TEMPERATURE (ºC)